Electronic structures of amorphous $Ni_{1-x}P_x$ glasses

W. Y. Ching
Department of Physics, University of Missouri—Kansas City, Kansas City, Missouri 64110-2499
(Received 21 January 1986; revised manuscript received 21 April 1986)

Electronic structures of amorphous $Ni_{1-x}P_x$ glasses for $x=0.25$, 0.20, and 0.15 are calculated with use of the orbital charge self-consistent orthogonalized linear combination of atomic orbitals method. Periodic structural models containing 100 atoms each are constructed first, using the Monte Carlo method. Results are presented for the total and partial density of states (DOS), joint DOS, localization index for each state, effective charges on each atom, and DOS at the Fermi level (E_F). The E_F is located at the steep edge of the Ni d band resulting in a Ni d-band hole in all three glasses. The local DOS of Ni atoms depends very sensitively on the number of P atoms as nearest neighbors while the local DOS of P atoms is rather insensitive to the atomic environment. For Ni atoms with no P atom as a nearest neighbor, its local DOS has a sharp peak above E_F and its effective charge is much reduced. Mulliken charge analysis indicates that on average, P atom gains about 0.4 to 0.8 electrons from Ni atoms for x ranges from 0.25 to 0.15. The average conduction electron per Ni atom is calculated to be 1.5 electron. The high resistivity of a-$Ni_{1-x}P_x$ glasses may be related to the existence of localized electron states near E_F.

I. INTRODUCTION

Of all the metallic glasses, Cu_xZr_{1-x} and $Ni_{1-x}P_x$ are probably the two most intensively studied.[1-5] The former belongs to a general class of transition-metal (TM) —TM glasses. To be more specific, Cu_xZr_{1-x} is formed by an early TM (Zr) and a late TM (Cu), and such combinations generally form metallic glasses very easily over a wide compositional range. $Ni_{1-x}P_x$, on the other hand, is a representative of another major class of metallic glasses, namely, the TM-metalloid glasses. In this series, the glass can only be formed in a very limited range of metalloid composition of about 15—25 at.% with the eutectic at about 17—18 at.%. Various structural,[6-12] physical,[13-16] electronic,[17-22] magnetic,[23-26] optical,[27,28] and transport properties[29,30,13,18,19,26] of $Ni_{1-x}P_x$ have been measured in the past. As the P concentration increases from 0.15 to 0.25, the resistivity increases and its temperature coefficient becomes negative and the thermoelectric power changes from negative to positive.[18,26,29-31] For glasses of the same x, it appears that the temperature coefficient is also dependent on the methods of sample preparation.[30] The glass is ferromagnetically ordered for $x<0.18$ but becomes paramagnetic for $x>0.18$.[26,30] Specific-heat measurements[13-16] indicate that the density of states (DOS) at the Fermi level, $N(E_F)$, decreases as x increases. The possibility of the existence of multiphase structures and a clustering effect in these glasses complicates the situation even further.[13,24,32,33] Numerous structural models have been built for TM-metalloid glasses with variable degrees of success,[8,10,12,34-37] and there has been no universally accepted criterion to characterize the short-range order (SRO) in this class of metallic glasses. Recently, Weber and Stillinger have made a very detailed investigation on the structure and kinetics of a-Ni-P alloys using molecular-dynamics simulations.[12] Several theories[38-48] have also been advanced to explain the existent experimental data. In contrast to the abundant experimental and theoretical work on $Ni_{1-x}P_x$ glass, there is very little direct information about the electronic structure of $Ni_{1-x}P_x$ which should be the basis of any theoretical interpretation of much of the experimental data. Messmer[49] studied the metalliod-metal interactions in $Fe_{40}Ni_{40}B_{20}$ and $Fe_{40}Ni_{40}P_{20}$ glasses by performing spin-polarized self-consistent-field $X\alpha$-scattered-wave calculations on small clusters. Fujiwara[50] calculated the DOS of $Fe_{1-x}B_x$ system using the linear combination of muffin-tin orbitals (LMTO) method. Kelley and Bullett[51] calculated the electronic structure of $Pd_{80}Si_{20}$ using a simplified tight-binding Hamiltonian, and Chowdhary *et al.*[52] used the two-component effective-medium approximation to study the electronic structures of amorphous Ni-B and Ni-P alloys.

In this paper we present detailed results on the electronic structures of $Ni_{1-x}Pa_x$ with $x=0.15$, 0.20, and 0.25 calculated by using the first-principles orthogonalized linear combination of atomic orbitals (OLCAO) method.[53] This method has recently been used to study the electronic structures of Cu_xZr_{1-x} glasses[54,55] with great success, and it is only natural that a similar calculation should be extended to the TM-metalloid and other metallic glasses. In this method both the topological and chemical disorder in the glass model can be treated accurately and the electronic structure of each individual atom can be analyzed and correlated with its local environment. Furthermore, the s, p, and d orbital components of the state densities and wave functions can be easily projected out. The most attractive part of the calculation is that each electronic state can be analyzed in terms of a localization index[55] (LI), which could provide great insight on the transport properties of these glasses. The calculations were performed on periodic models containing a total of 100 atoms each constructed by means of Monte Carlo method, and, in the present case, we have further implemented an orbital-

charge—self-consistent scheme[56] within the OLCAO method to improve accuracy. A comparative study of the electronic structures of crystalline Ni_3P (c-Ni_3P) and amorphous $Ni_{75}P_{25}$ (a-$Ni_{75}P_{25}$) based on a non-self-consistent calculation was presented earlier.[57] Based on the calculated electronic structure, attempts to correlate the theoretical results with the SRO in the structures and experimental data were made.

In the following section, we will briefly outline the procedure and the method of our calculation. Results are presented and discussed in Sec. III, where comparisons with experiments are also made whenever appropriate. These results and possible extension of our first-principles approach to study the structures and properties of amorphous solids are further discussed in the last section.

II. METHOD

The method of our calculation is described in the earlier paper on Cu_xZr_{1-x} glass[55] and only a brief outline will be presented here. Quasiperiodic models with 100 atoms in a cubic cell were constructed using the Monte Carlo method[58] with pairwise central-force potentials. Close contacts between metalloid and metalloid pairs were avoided by proper choice of initial atomic positions. The size of the cell is determined by the mass density of the specific glass and the periodic boundary condition is imposed. Three models with $x=0.25$, 0.20, and 0.15 were constructed. To calculate the electronic structures of these glass models, atomiclike potential functions to be centered at each atomic site were first constructed for Ni and P atoms, respectively, according to the usual local-density-functional theory with an exchange parameter of 0.71. Minimal atomiclike basis functions were contracted from the atomiclike potentials with a set of 14 Gaussian orbitals. Good band structures and DOS's were obtained for the crystalline Ni using these potentials and basis functions even though the dimension of the matrix equation involved is only 9×9.[56,57] Because of this economic use of basis in the OLCAO method, we were able to use the same potential and basis functions to calculate the electronic structures of $Ni_{1-x}P_x$ glasses. Because both the atomiclike basis functions and the atomiclike potentials were expanded in terms of Gaussian-type orbitals, all the multicenter integrals occurring in the Hamiltonian and the overlap matrix elements can be evaluated exactly. After orthogonalization to the core procedure, each Ni atom has only nine orbitals ($4s$, $4p_x$, $4p_y$, $4p_z$, $3d_{xy}$, $3d_{yz}$, $3d_{zx}$, $3d_{x^2-y^2}$, and $3d_{3r^2-z^2}$) and each P atom retains only four orbitals ($3s$, $3p_x$, $3p_y$, and $3p_z$), so the dimension of the matrix equations in our calculation ranges from 775 in $Ni_{75}P_{25}$ to 825 in $Ni_{85}P_{15}$. The energy eigenvalues and eigenvectors were obtained by direct diagonalization of the secular equation at the center of the small quasi-Brillouin-zone. To start an orbital-charge—self-consistent procedure, the Mulliken charge on each orbital of each atom was calculated from the wave functions and used to adjust the diagonal Hamiltonian matrix elements for the next iterative calculation.[56] Iteration stops when the change in Mulliken charge on each atom stabilizes to less than 0.01 electron per atom. In principle, a procedure to include the variation of the off-diagonal Hamiltonian matrix elements in the self-consistent scheme can be worked out. However, in an amorphous structure, we found the effect of changing the off-diagonal elements in the self-consistent cycle is quite small; therefore such a procedure is not implemented in the present calculation.

The LI for the state m is calculated from the orbital charge $\rho^m_{i,\alpha}$ on each atomic site α:

$$L_m=\sum_{\alpha,1}(\rho^m_{i,\alpha})^2 , \tag{1}$$

where

$$\rho^m_{i,\alpha}=\sum_{j,\beta}C^m_{i\alpha}C^m_{j\beta}S_{i\alpha,j\beta} . \tag{2}$$

$C^m_{i\alpha}$ are the eigenvector coefficients and $S_{i\alpha,j\beta}$ are the overlap matrix elements between i and j orbitals of atoms centered at sites α and β, respectively.

III. RESULTS

A. Analysis of models

Our models for $Ni_{1-x}P_x$ glasses with only 100 atoms each are admittedly small and may not be appropriate for glasses in which higher structural order exists. Nevertheless, they provide the basis on which detailed electronic structure can be calculated using a first-principles approach. In Table I we list the parameters of the pair potentials,

$$V_{ij}=\begin{cases} A/r_{ij}^{12}+B/r_{ij}^{6}+Cr_{ij}+D & \text{for } 0<r_{ij}\le r_t, \\ 0 & \text{for } r_{ij}>r_t, \end{cases} \tag{3}$$

used in the construction of the models by the Monte Carlo method. r_{ij} is the distance between atoms i and j, and r_t is the truncation distance. These potentials were obtained from the bulk properties of Ni and P (Ref. 34) and were cast in a modified Lennard-Jones form.[55] All the structural information about these models are tabulated in Table II, including the chemical short-range order η_{AB} for a two-component glass as defined by Cargill and Spaepen.[59] Also listed are the generalized Warren chemical SRO parameter[10,60] defined as

$$\alpha_W=Z_{cc}/Z_W , \tag{4}$$

where

$$Z_{cc}=x(Z_{NiNi}-Z_{PNi})+(1-x)(Z_{PP}-Z_{NiP}) ,$$

$$Z_W=xZ_{Ni}+(1-x)Z_P .$$

Z_{ij} is the number of average j-type nearest-neighbors (NN's) to i-type atoms and $Z_i=Z_{ij}$. It is apparent that substantial SRO exists in these models as the result of no P-P contact in these models. For $Ni_{80}P_{20}$ we have $\alpha_W=-0.153$, which is in very good agreement with the value of -0.144 obtained by Harris and Lewis[10] and the experimental value of -0.15. In Cu_xZr_{1-x} models there is virtually no chemical SRO.[55] The radial distribution functions (RDF's) of the three models and their partial

TABLE I. Parameters of modified Lennard-Jones potential, and truncation distances R_T used in the Monte Carlo modeling of $Ni_{1-x}P_x$.

Pair	A (eV Å^{-12})	B (eV Å^{-6})	C (eV Å^{-1})	D (eV)	R_T (Å)
Ni-Ni	0.4771×10^5	-0.5368×10^3	-0.00377	0.0286	6.5
Ni-P	0.1948×10^5	-0.2374×10^3	-0.00570	0.0393	6.5
P-P	0.5368×10^6	-0.5367×10^3	-0.00078	0.0081	6.5

components are presented in Fig. 1. The sharp first peak and the split second peak are characteristics of a two-component glass. These RDF's are in reasonable agreement with experiment[6,7] and no further attempts were made to improve the agreement. In order to analyze the electronic structure of $Ni_{1-x}P_x$ according to the local environment of each atom and for a reason which becomes apparent later, we divide the Ni atoms in each model into seven different groups, Ni_n, where $n=0,1,2,3,4,5,6$ is the number of nearest-neighbor P atoms. Likewise, the P atoms are also divided into different groups according to the number of total NN's. (For that purpose, the NN distance is taken to be the first minimum in the RDF of each model.) The distributions of Ni and P atoms in the three models and an equivalent model for the tetragonal c-Ni_3P according to this classification are shown in Fig. 2. It is apparent that in our models there are hardly any P atoms with twelve NN's, indicating that the icosahedral type of SRO (Refs. 61 and 62) is not present in these models; the distributions in c-Ni_3P and a-$Ni_{75}P_{25}$ are substantially different although the composition ratios of the two phases are the same. We also note that as P content increases, the number of Ni atoms with 0 or 1 P NN decreases.

B. Electron DOS and partial DOS

In Figs. 3(a)–3(c) we display the calculated total and partial DOS (PDOS) of $Ni_{1-x}P_x$ for $x=0.25$, 0.20, and 0.15, respectively. The dependence of DOS on x is not strong and in all three cases the DOS is dominated by the Ni d peak. The E_f intersects at the steep low-energy side of the Ni d band, resulting in the preservation of the Ni d band hole. This result is in complete agreement with the $L_{III,II}$ edge x-ray-absorption near-edge-structure measurement on electrodeposited a-$Ni_{1-x}P_x$ samples by Choi *et al.*,[21] but is in variance with the arguments based on a rigid-band model.[20] The Ni d band peaks at about -2.0 eV. The P bands are located at much lower energy. The P $3s$ band ranges from -16 to -12 eV and the P $3p$ band which consists of a double-peak structure ranges from -10 to -5 eV just below the Ni d band. Above the Ni d peak there are no prominent structures in the DOS. These DOS features are quite different from the TM-TM glasses such as Cu_xZr_{1-x},[55] where the structures in the DOS are controlled by the relative positions of the d bands of the two TM's. From the orbital-projected PDOS, it can be concluded that there are substantial hybridization effects between P_{3s} and Ni_{4s} orbitals and between P $2p$, Ni $4p$, and Ni $3d$ orbitals. As x decreases, the structures move to higher binding energy. This shift is nonlinear in x since there appears to be a much bigger shift from $x=0.25$ to 0.20 than from $x=0.20$ to 0.15. The calculated DOS is in general agreement with the x-ray-photoelectron-spectroscopy measurement,[22] but the experimental data do not have high enough resolution for a more critical comparison. The double peak structure of the P $2p$ band between -10 and -5 eV is also in agreement with the soft-x-ray $K\beta$ emission measurement[20,21] on Ni-P alloys.

In contrast to the insensitive dependence of the total DOS on x, the local DOS (LDOS) per Ni atom depends very sensitively on its local environment, such as the number of P atoms that are NN's. In Figs. 4(a)–4(c) we display the PDOS per Ni atom in a-$Ni_{1-x}P_x$ according to different groups displayed in Fig. 2. For Ni atoms with

TABLE II. Supercell lattice constant a, NN distance r_{min}, average coordination number, and SRO parameters.

	$Ni_{75}P_{25}$	$Ni_{80}P_{20}$	$Ni_{85}P_{15}$
x	0.25	0.20	0.15
a (Å)	10.3551	10.3536	10.3538
r_{min} (Å)	2.96	2.98	3.00
Z_{NiNi}	8.213	9.275	9.647
Z_{NiP}	3.000	2.350	1.788
Z_{Ni}	11.213	11.625	11.435
Z_{PP}	0.080	0.211	0.143
Z_{PNi}	9.000	9.895	10.857
Z_P	9.080	10.105	11.000
η_{NiNi}	-0.070	-0.029	-0.013
η_{PP}	-0.959	-0.883	-0.911
η_{NiP}	0.259	0.132	0.078
Z_{cc}	-2.368	-1.589	-1.576
Z_W	9.613	10.414	11.066
α_W	-0.246	-0.153	-0.142

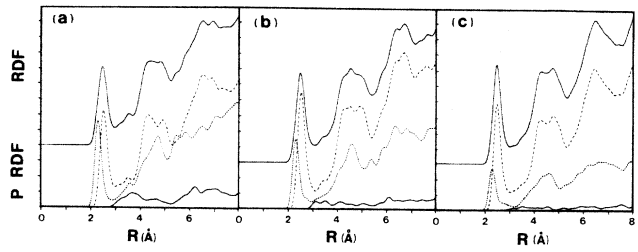

FIG. 1. Total RDF and partial RDF (lower panel: solid line, P-P; dotted line, Ni-P; dashed line, Ni-Ni). (a) $Ni_{75}P_{25}$; (b) $Ni_{80}P_{20}$; (c) $Ni_{85}P_{15}$.

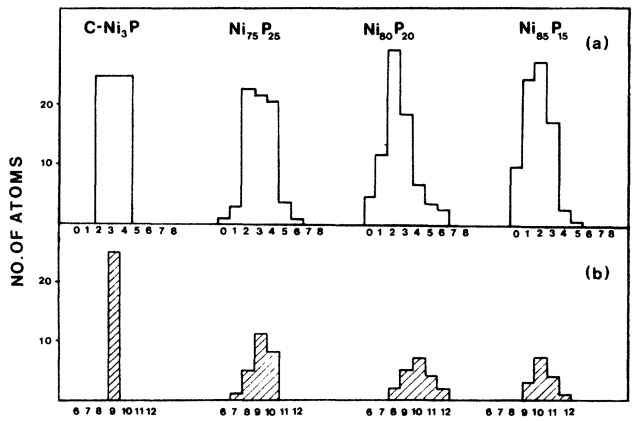

FIG. 2. Distribution of atoms in 100 atoms models for $Ni_{75}P_{25}$, $Ni_{80}P_{20}$, $Ni_{85}P_{15}$, and an equivalent model of tetragonal crystal of Ni_3P. (a) Ni atoms according to number of nearest P neighbors; (b) P atoms according to number of total nearest neighbors.

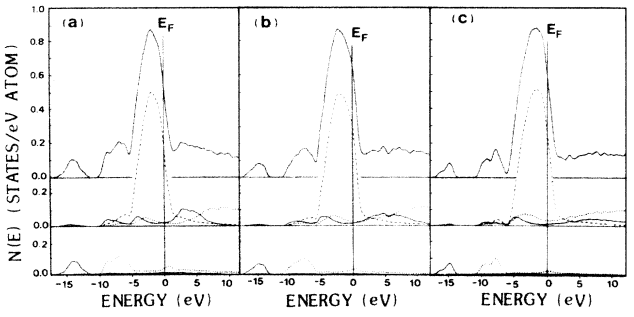

FIG. 3. DOS of (a) $Ni_{75}P_{25}$, (b) $Ni_{80}P_{20}$, and (c) $Ni_{85}P_{25}$: upper panel, total; middle panel, PDOS; solid line, Ni $4s$; dotted line, Ni $4p$; dashed line, Ni $3d$; lower panel PDOS, solid line, P $3s$; dotted line, P $3p$.

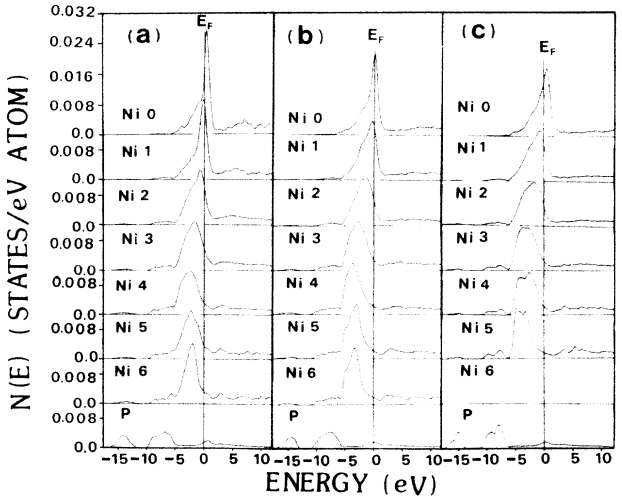

FIG. 4. DOS per atom for Ni_n and P: (a) $Ni_{75}P_{25}$; (b) $Ni_{80}P_{20}$; (c) $Ni_{85}P_{15}$.

no P atom as a NN, the PDOS has a very sharp peak above or close to E_F; as the number of P NN's is increased from 1 to 4, the peak becomes less sharp and shifts to lower energy (higher binding energy). However, when n increases from 5 to 6, the peak again becomes sharper and shifts slightly backward. This sensitive dependence of the LDOS of the Ni atom on its particular local environment is not surprising; the P atom has a lower electronic energy than the Ni atom, as can be seen from the locations of the relative peak positions in the PDOS in Fig. 3. A Ni atom with no P as a NN will feel a higher potential energy in comparison with other average Ni atoms. These Ni atoms, which are relatively few, can be viewed as "impuritylike" atoms in the amorphous Ni-P environment. They have sharp DOS peaks above or close to E_F and are responsible for the preservation of the Ni d-band hole. On the other hand, the PDOS of P atoms show very little variation with respect to the different number of Ni atoms as NN's (Fig. 2). This is primarily because the P states are rather deep and more localized; they are less sensitive to the local potential fluctuations due to the chemical as well as topological disorder.

C. Localization index of electron states

One of the advantages of the first-principles OLCAO method is that each electron state can be analyzed in terms of a LI calculated from its wave functions. The charge of an electron with energy E_n can be divided among various orbitals of all the atoms in the cubic cell according to the Mulliken scheme.[63] The LI calculated in this manner gives a very realistic estimation of the extended or localized nature of electronic states in a disordered system across the entire energy range. In Figs. 5(a)—5(c) we plot the LI of each state against its energy E_n for the three glasses with $x=0.25$, 0.20, and 0.15, respectively. It is clear that P $3s$ and P $3p$ states with relatively high binding energy are very localized, and states in the middle of the Ni $3d$ band are relatively delocalized while those at the edges are relatively localized. The unoccupied conduction-band states about 1 eV above E_F are completely delocalized. In metallic systems, states close to the Fermi surface are the most important in determining the transport properties; it is therefore necessary to examine these states more closely. In the insets of Fig. 5, we replot th LI of states within 2 eV of E_F on an expanded scale. There exist localized states within 1 eV above E_F for all three glasses. These localized states are the states at the edges of the Ni d band and most likely originate from the Ni atoms with 0 or 1 P atom as a NN that have been discussed earlier. Because of their proximity to E_F, these states will definitely affect the transport properties of these glasses and may be related to the high resistivity of $Ni_{1-x}P_x$ glasses. We may recall that in the case of Cu_xZr_{1-x} glasses[55] the states near E_F are delocalized because E_F is located on a plateau of a very wide Zr d band. In the case of Ni_xP_{1-x} glasses E_F is located at the steep edge of a relatively narrow Ni d band. Our models for Ni_xP_{1-x} are not big enough to produce a statistically large enough number of localized states above E_F for a

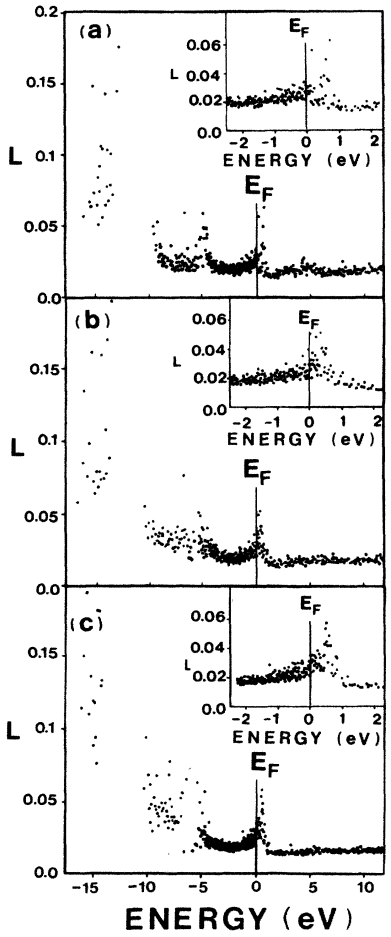

FIG. 5. Localization index for all eigenstates in (a) $Ni_{75}P_{25}$; (b) $Ni_{80}P_{20}$; (c) $Ni_{85}P_{15}$. Inset, LI for states near E_F.

more detailed analysis; however, the degree of localization of these states seems to depend on x, which, in turn, affects the microscopic atomic-scale structures. It is not straightforward to correlated the x dependence of conductivity or thermoelectric power to the LI calculated here. In principle, when the conductivity or the resistivity of each glass is calculated in a first-principles manner from the Kubo-Greenwood formula,[64] the effect of the localized nature of these states will be reflected in the matrix elements formed by the wave functions of these states. Such detailed calculations in metallic glasses have not yet been realized, although simplified calculations along this line have been attempted, giving very reasonable results.[47]

D. Joint density of states

McKnight and Ibrahim[27] have measured the infrared reflection on $Ni_{1-x}P_x$ glasses for x ranging from 0.15 to 0.26 for photon energy up to 2.5 eV. They concluded that for $x=0.152$ and 0.186, the Drude-type intraband transition is not a good model for frequencies greater than 0.7 eV, but for $x=0.211$ and 0.262 the Drude approximation is good up to 1.5 eV. The same optical data also indicate that the interband transitions occur at higher frequencies as x is increased. In the constant-matrix approximation, the interband contribution to the optical conductivity can be approximated by the joint DOS (JDOS). In the metallic glass system the constant-matrix approximation should be a reasonable one because the electron states have no **k** dependence and the DOS generally lacks any sharp structures derived from the van Hove singularities. We have calculated the JDOS for $Ni_{1-x}P_x$ for photon frequencies up to 20 eV and these are shown in Fig. 6. The double-hump structures between 4 and 10 eV are the reflections of the occupied Ni $3d$ and P $3p$ peaks in the DOS since the conduction-band DOS's are relatively featureless. In the intermediate-frequency range of 1—3 eV, where the interband transitions begin to dominate, the JDOS increases as x decreases (see inset of Fig. 6), which is in line with the observation of Ref. 27; but beyond 3 eV this trend is reversed. It will be highly interesting to extend the optical measurement to higher-frequency ranges and to check whether the relative strengths of absorption for different x will be reversed as predicted by our JDOS calculations. On the other hand, it will also be desirable to include the effect of matrix elements in calculating the interband optical transitions and to ascertain the role played by the relatively localized states near E_F.

E. Effective charges

In Figs. 7(a)—7(c) we display the distribution of effective charges on the 100 atoms in the three models calculated according to the Mulliken scheme.[63] In all cases, the P charges show very small variation from atom to atom with an average value of 5.38, 5.63, and 5.78 electrons for $x=0.25$, 0.20, and 0.15, respectively, while the effective charges on Ni atoms show a wide range of distribution ranging from 5 to 11 electrons. Effective charges as low as 4.8 electrons can be found, which corresponds to Ni_0-type atoms near E_F. The average charge per Ni atom is found to be 9.87, 9.84, and 9.86 electrons for $x=0.25$, 0.20, and 0.15, respectively. Thus, on the average, charges are transferred from Ni atoms to P atoms. This is in complete variance with the rigid-band model[65] which predicts that *electrons are transfered from the P atom to fill the Ni—band hole.* Our first-principles calculation indicates that this is not true. In a free-electron-type theory,

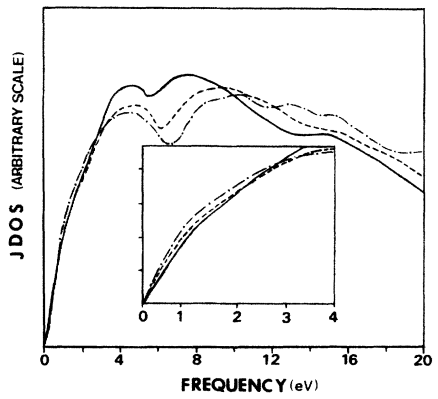

FIG. 6. JDOS of $Ni_{1-x}P_x$ in arbitrary unit. Insect, JDOS in the frequency range 0—4 eV. Solid line, $Ni_{75}P_{25}$; dashed line, $Ni_{80}P_{20}$; dashed-dotted line, $Ni_{85}P_{15}$.

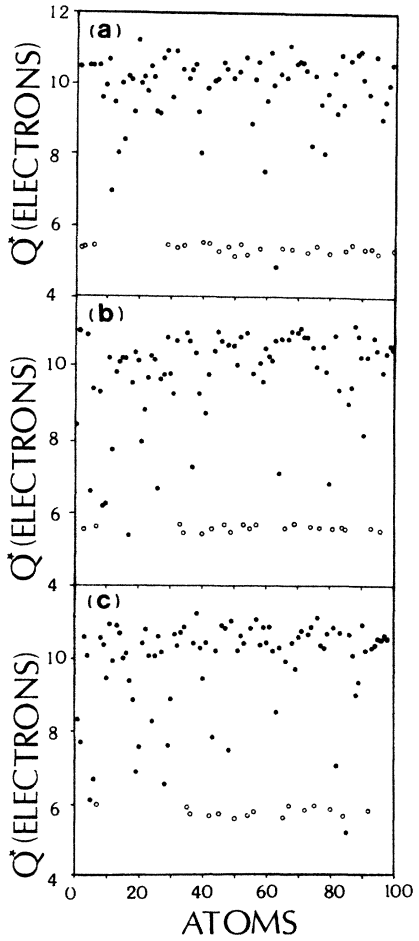

FIG. 7. Effective charges per atom in $Ni_{1-x}P_x$. Solid circle, Ni atom; open circle, P atom. (a) $Ni_{75}P_{25}$; (b) $Ni_{80}P_{20}$; (c) $Ni_{85}P_{15}$.

such as that of Ziman,[66] Ziman and Faber,[67] or the latter's extension,[68] the number of conduction electrons per Ni atom is a very important parameter and its accurate value has not been confidently established. If we assume that the s,p electrons in Ni atoms are the conduction electrons and the d electrons are the localized electrons, then the average number of conduction electrons in $Ni_{1-x}P_x$ glass per Ni atom from our calculation is 1.46, 1.48, and 1.45 for $x=0.25$, 0.20, and 0.15, respectively. This is surprisingly close to the effective valence assumed for the a-$Ni_{1-x}P_x$ system in the study of electric resistivity using the diffraction model.[18] However, the LI calculation indicates that the states in the middle of the Ni d band may not be completely localized and it is open to debate whether these states should be taken into consideration as well. These results are summarized in Table III.

F. DOS at the Fermi level

Another very important quantity in relation to transport properties of $Ni_{1-x}P_x$ glasses is the DOS at the Fermi level, $N(E_F)$. It is related to the conductivity though $\sigma=e^2N(E_F)D$, where D is the electron diffusivity. $N(E_F)$ can also be extracted from the specific-heat data, and it was found that as x increases the $N(E_F)$ decreases in the $Ni_{1-x}P_x$ series.[13–15,17] According to Mott's s-d scattering theory,[69] the resitivity of a metallic glass is proportional to the density of d electrons at E_F, $N_d(E_F)$, and only the s,p components of $N(E_F)$ contribute to conductivity; it is therefore important to project out the $N(E_F)$ values according to different orbital components. Our calculated values of $N(E_F)$ and its resolution into different orbital components are also listed in Table III. It is obvious that $N(E_F)$ is dominated by the Ni d states with negligible P contribution. This is consistent with the experimental finding that the value of the Knight shift,[24] as seen at the P site, is insensitive to x. The calculated total $N(E_F)$ is in general agreement with values deduced from the specific-heat data[14,17] for both a-$Ni_{1-x}P_x$ and c-Ni_3P, and this is shown in Fig. 8. The $N(E_F)$ values for $Ni_{80}P_{14}B_6$, $Ni_{80}P_{12}B_8$, and $Ni_{78}P_{14}B_8$ glasses deduced from specific-heat data are about 25—30% larger than our calculated value for $Ni_{80}P_{20}$.[16] This is probably due to the fact the the presence of B increases $N(E_F)$ because B has a higher atomic energy than P and therefore interacts more strongly with the Ni d band. For $x\leq 0.18$, $Ni_{1-x}P_x$ is weakly ferromagnetic and our paramagnetic

TABLE III. DOS at E_F and effective atomic charges Q^* in $Ni_{1-x}P_x$ glasses.

		$Ni_{75}P_{25}$	$Ni_{80}P_{20}$	$Ni_{85}P_{15}$
$N(E_F)$ (states per eV per atom)	Ni 4s	0.017	0.018	0.013
	Ni 4p	0.018	0.021	0.026
	Ni 3d	0.495	0.551	0.565
	P 3s	0.007	0.004	0.004
	P 3p	0.030	0.024	0.019
	Total	0.567	0.618	0.626
Q^* (electrons)	Ni 4s	0.831	0.745	0.607
	Ni 4p	0.634	0.737	0.845
	Ni 3d	8.408	8.362	8.411
	Average Ni	9.873	9.844	9.863
	P 3s	1.680	1.682	1.653
	P 3p	3.702	3.943	4.124
	Average P	5.382	5.625	5.777

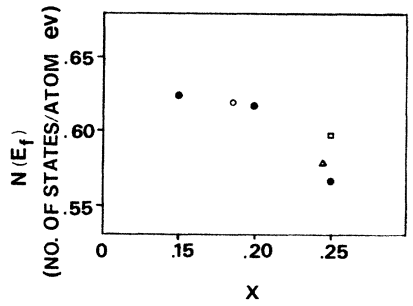

FIG. 8. DOS at E_F, solid circle, this calculation; open square, experimental data for c-Ni_3P, Ref. 22; open triangle, experimental data of Ref. 17; open circle, experimental data of Ref. 14 [corrected for s,p contribution of the majority spin according to $N(E_F)=N_\downarrow(E_f)+N^\uparrow(E_F)\approx 1.20N_\downarrow(E_F)$].

calculation can only provide a qualitative estimate for $N(E_F)$. It should also be pointed out that because E_F intersects the very steep side of the Ni d band, our calculated absolute values for $N(E_F)$ may be subject to some degree of uncertainty. To obtain more accurate values of $N(E_F)$ at different x, calculations on several models with the same x may be performed to obtain more reliable average values.

Based on a free-electron model, Nagel and Tauc[40] had argued that the stability of a two-component glass such as $Ni_{1-x}P_x$ is related to the fact that E_F is located at a local minimum in the DOS. Such is not the case with $Ni_{1-x}P_x$ glasses, since the calculated E_F is at the steep edge of the huge Ni d peak. However, the s,p part of the DOS does show a broad minimum at about 1 eV below E_F, as illustrated in Fig. 9 for the three glasses. Because $N(E_F)$ is dominated by Ni d states especially at the Fermi level, it is concluded that a free-electron-like theory is inadequate to explain the glass stability in metal-metalloid glasses.

IV. DISCUSSION

Our primary goal in this paper is to provide detailed information about the electronic structure of the $Ni_{1-x}P_x$ glasses. The first-principles nature of the calculation enables us to study the disorder and the short-range order in metallic glasses at the microscopic level. The results obtained on the $Ni_{1-x}P_x$ glasses are in general agreement with a variety of experiments and can be summarized as follows: (1) The DOS is dominated by the Ni d band and the metalloid atom states are much lower in energy. (2) Substantial chemical bonding exists between Ni and P atoms and the Ni d-band hole is preserved. (3) The local DOS of Ni atoms depends very sensitively on the number of P atoms as nearest neighbors, while the local DOS of P atoms is rather insensitive to the atomic environment. (4) There exist relatively localized states about 1 eV above E_F which may play an important role in the transport properties of the $Ni_{1-x}P_x$ glasses. (5) The calculated JDOS is consistent with optical experiment. (6) The DOS at the Fermi level is dominated by the Ni d band and is in general agreement with the values derived from the specific-heat data. (7) Charges are transferred from Ni to P atoms and the calculated average conduction electron per Ni atom is 1.5 electron. (8) Our results do not support the free-electron-model— or the rigid-band-model—type theory for $Ni_{1-x}P_x$ glasses.

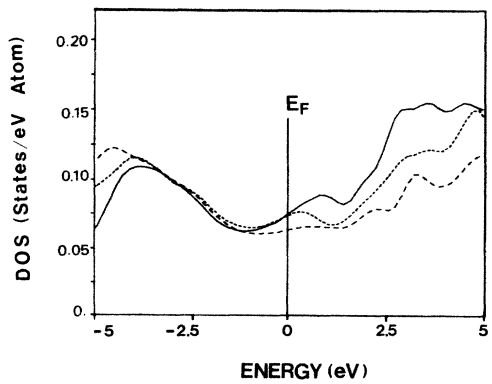

FIG. 9. DOS of s,p electrons near E_F: solid line, $Ni_{75}P_{25}$; dotted line, $Ni_{80}P_{20}$; dashed line, $Ni_{85}P_{15}$.

In studying the electronic structures of metallic glasses, we must bear in mind that the atomic-scale SRO in a system such as $Ni_{1-x}P_x$ glassses is very complicated and may involve the existence of several different phases. Our model structures, constructed by using the Monte Carlo method with reasonable interatomic pair potentials, give satisfactory RDF's. This does not mean that these models are necessarily correct since the RDF only provides a spatially averaged distribution of atomic positions. What our calculation can provide is another type of topological data of high quality, because the LDOS of each type of atom depends very sensitively on its SRO. This sensitive dependence of LDOS on the atomic environment provides a very useful tool for delineating the subtle features in the electronic structure of glass systems. It is conceivable that one may be able to build specific SRO (such as icosahedral order[61,62]) regions of polycrystalline phases, clustering effect, or low-barrier bistable configurations[12] into the model structure and study their consequences on the electronic structure. However, much larger models must be built and such calculations will be computationally more demanding. It is also possible to use the electron wave functions obtained from the present calculation to perform accurate transport-property calculations. Another exciting approach is to combine the molecular-dynamics simulations for the structure with the local-density-functional theory for the electronic-structure calculation to study the fundamental properties of the condensed systems.[70] When such studies are carried out systematically on a very large number of different metallic glasses, a much more complete understanding about the structures and properties of metallic glasses can be achieved.

ACKNOWLEDGMENTS

This work was supported by U.S. Department of Energy under Contract No. DE-FG02-84ER45170. The assistance of L. W. Song in the construction of models used in the present calculation is gratefully acknowledged.

[1]See, for example *Glassy Metals I and II*, edited by H.-J. Güntherodt and H. Bec (Springer-Verlag, New York, 1981 and 1983).
[2]*Glassy Metals: Magnetic, Chemical and Structural Properties*, edited by R. Hasegawa (Critical Review in Chemistry, 1983).
[3]S. R. Nagel, Adv. Chem. Phys. **51**, 227 (1982).
[4]U. Mizutani, Prog. Mater. Sci. **28**, 97 (1983).
[5]D. G. Nagle, J. Phys. Chem. Solids **45**, 367 (1984).
[6]G. S. Cargill III, J. Appl. Phys. **41**, 12 (1970).
[7]Y. Waseda and S. Tamaki, Z. Phys. B **23**, 315 (1976).
[8]J. F. Sadoc and J. Dixmier, Mater. Sci. Eng. **23**, 187 (1976).
[9]E. Vafari-Makhsoos, E. L. Thomas, and L. E. Toth, Metall. Trans. A **9**, 1449 (1978).
[10]R. Harris and L. J. Lewis, Phys. Rev. B **25**, 4997 (1982); J. Phys. F **13**, 1359 (1983).
[11]F. Machizaud, F. A. Kuhnast, and J. Flechon, J. Non-Cryst. Solids **68**, 271 (1984).
[12]T. A. Weber and F. H. Stillinger, Phys. Rev. B **31**, 1954 (1985); **32**, 5402 (1985).
[13]Y. S. Tyan and L. E. Toth, J. Electron. Mater. **3**, 791 (1974).
[14]R. Kuentzler, I. Bakonyi, and A. Lovas, Solid State Commun. **55**, 567 (1985).
[15]C. Cohen *et al.*, Phys. Rev. B **31**, 5 (1985).
[16]T. A. Donnelly, T. Egami, and D. G. Onn, Phys. Rev. B **20**, 1211 (1979).
[17]P. J. Cote, G. P. Capsimalis, and G. L. Salinger, in *Amorphous Magnetism II*, edited by R. A. Levy and R. Hasegawa (Plenum, New York, 1977), p. 499.
[18]P. J. Cote, Solid State Commun. **18**, 1311 (1976); P. J. Cote and L. V. Meisel, Phys. Rev. B **20**, 3030 (1979).
[19]E. Belin, C. Bonnelle, J. Flechon, and F. Machizaud, J. Non-Cryst. Solids **41**, 219 (1980); E. Belin, C. Bonnelle, S. Zuckerman, and F. Machizaud, J. Phys. F **14**, 625 (1984).
[20]W. H. Hines, C. U. Modzelewski, R. N. Paolino, and R. Hasegawa, Solid State Commun. **39**, 699 (1981).
[21]M. Choi, D. M. Pease, W. A. Hines, G. H. Hayes, J. I. Budnick, S. M. Heald, R. Hasegawa, and H. E. Schone, Phys. Rev. B **32**, 7670 (1985).
[22]A. Amanou, D. Aliaga-Guerra, P. Panissod, G. Krill, and R. Kuentzler, J. Phys. (Paris) Colloq. **41**, C8-396 (1986).
[23]I. Bakoryi, L. K. Varga, A. Lovas, E. Togh-Kadar, and A. Solyóm, J. Magn. Magn. Mater. **50**, 111 (1985).
[24]L. H. Bennett, H. E. Schone, and P. Gustafson, Phys. Rev. B **18**, 2027 (1978).
[25]T. Egami, Rep. Prog. Phys. **47**, 1601 (1984).
[26]A. Berrada, L. M. Lapierre, B. Loegel, P. Panissod, and C. Robert, J. Phys. F **8**, 845 (1978).
[27]S. W. McKnight and A. K. Ibrahim, Phys. Rev. B **29**, 6570 (1984).
[28]J. Rivory, B. Bouchet, and Y. Bertraud, J. Phys. (Paris) Colloq. **41**, C8-430 (1980).
[29]L. Mendoza-Zelis, L. Thome, L. Brossard, J. Chaummont, K. Krolas, and H. Bernas, Phys. Rev. B **26**, 1306 (1982).
[30]J. P. Carini, S. R. Nagel, L. K. Varga, and T. Schmidt, Phys. Rev. B **27**, 7589 (1983).
[31]L. Thome, A. Traverse, and H. Bernas, Phys. Rev. B **28**, 6523 (1983).
[32]D. S. Lashmore, L. H. Bennett, H. E. Schone, P. Gustafson, and R. E. Watson, Phys. Rev. Lett. **48**, 1760 (1982).
[33]R. E. Watson, L. M. Bennet, in *Proceedings of the International Conference on Magnetism*, edited by J. J. Rhyne *et al.* (North-Holland, Amsterdam, 1986), p. 295.
[34]W. Y. Ching and C. C. Lin, *Amorphous Magnetism II*, Ref. 17, p. 469.
[35]A. Rahman, M. J. Mandell, and J. P. McTague, J. Chem. Phys. **64**, 1564 (1976).
[36]D. S. Boudreaux and H. J. Frost, Phys. Rev. B **23**, 1506 (1981).
[37]F. Lancon, L. Billard, J. Langier, and A. Chamberod, J. Phys. F **12**, 259 (1982).
[38]O. Dreirach, R. Evans, H.-J. Güntherodt, and H. V. Kunzi, J. Phys. F **2**, 709 (1970).
[39]R. W. Cochrane, R. Harris, J. O. Strom-Olson, and M. J. Zuckerman, Phys. Rev. Lett. **35**, 676 (1975).
[40]S. R. Nagel and J. Tauc, Phys. Rev. Lett. **35**, 380 (1975).
[41]P. J. Cote and L. V. Meisel, Phys. Rev. Lett. **39**, 102 (1977).
[42]E. Esposito, H. Ehrenreich, and C. D. Gelatt, Jr., Phys. Rev. B **18**, 3913 (1978).
[43]S. M. Girvin and M. Jonson, Phys. Rev. B **22**, 3583 (1980).
[44]Y. Imry, Phys. Rev. Lett. **44**, 469 (1980).
[45]D. Nicholson and L. Schwartz, Phys. Rev. Lett. **49**, 1050 (1982).
[46]M. A. Howson, J. Phys. F **14**, L25 (1984).
[47]L. E. Ballentine and J. E. Hammerberg, Can. J. Phys. **62**, 692 (1984).
[48]R. W. Cochrane and J. O. Strom-Olson, Phys. Rev. B **29**, 1088 (1984).
[49]R. P. Messmer, Phys. Rev. B **23**, 1616 (1981).
[50]T. Fujiwara, J. Phys. F **12**, 661 (1982).
[51]M. J. Kelley and D. W. Bullett. J. Phys. C **12**, 2531 (1979).
[52]A. Chowdhary, D. M. Nicholson, and L. M. Schwartz, J. Non-Cryst. Solids **76**, 147 (1985).
[53]W. Y. Ching and C. C. Lin, Phys. Rev. B **12**, 5536 (1975); **16**, 2989 (1977).
[54]S. S. Jaswal and W. Y. Ching, Phys. Rev. B **26**, 1064 (1982).
[55]W. Y. Ching, L. W. Song, and S. S. Jaswal, Phys. Rev. B **30**, 544 (1984).
[56]W. Y. Ching, Solid State State Commun. **57**, 385 (1986).
[57]W. Y. Ching, J. Non-Cryst. Solids, **75**, 379 (1985).
[58]N. Metropolis, A. W. Rosenbluth, M. N. Rosenbluth, A. H. Teller, and E. Teller, J. Chem. Phys. **21**, 1087 (1953).
[59]G. S. Cargill III and F. Spaepen, J. Non-Cryst. Solids **43**, 91 (1981).
[60]B. E. Warren, in *X-Ray Diffractions* (Addison-Wesley, Reading, Mass., 1969).
[61]J. F. Sadoc, J. Non-Cryst. Solids **44**, 1 (1981).
[62]D. R. Nelson, Phys. Rev. Lett. **50**, 982 (1983).
[63]R. S. Mulliken, J. Chem. Phys. **23**, 1833 (1955).
[64]R. Kubo, Can. J. Phys. **34**, 1274 (1956); D. A. Greenwood, Proc. Phys. Soc. London **71**, 585 (1973).
[65]D. E. Polk, Scr. Metall. **4**, 117 (1970).
[66]M. Ziman, Philos. Mag. **6**, 1031 (1961).
[67]T. E. Faber and J. M. Ziman, Philos. Mag. **11**, 153 (1965).
[68]R. Evans, D. A. Greenwood, and P. Lloyd, Phys. Lett. **35A**, 57 (1971).
[69]N. F. Mott. Philos. Mag. **26**, 1249 (1972).
[70]R. Car and M. Parrinello, Phys. Rev. Lett. **55**, 2471 (1985).